Thermal Decomposition of Silicon-rich Oxides Deposited by the LPCVD Method[†]

Davor Ristić,[a] Mile Ivanda,[b,*] Krešimir Furić,[b] Alessandro Chiasera,[a] Enrico Moser,[c] and Maurizio Ferrari[a]

[a]*CNR-IFN, Istituto di Fotonica e Nanotecnologie, CSMFO Lab, via alla Cascata 56/C,Povo, 38123, Italy*
[b]*Ruđer Bošković Institute, Bijenička cesta 54, 10000 Zagreb, Croatia*
[c]*Nanoscience Laboratory, Department of Physics, University of Trento, Via Sommarive 14, Povo 38123, Italy*

Abstract. Silicon-rich oxide (SiO_x, $0 < x < 2$) thin films were deposited using the Low Pressure Chemical Vapor Deposition (LPCVD) method at temperature of 570 °C using silane (SiH_4) and oxygen as the reactant gasses. The films were annealed at temperatures of 800, 900, 1000, and 1100 °C to induce the separation of excess silicon in the SiO_x films into nanosized crystalline silicon particles inside an amorphous SiO_x matrix. The size of the silicon particles was determined using Raman spectroscopy. (doi: 10.5562/cca1969)

Keywords: LPCVD, silicon, thermal decomposition, thin films

INTRODUCTION

The optical properties of nanocrystalline silicon are very different than the properties of bulk silicon. While bulk silicon is a poor light emitter, nonocrystalline silicon was found to exhibit luminescence.[1] Among different methods to produce nanocrystalline silicon, one of the most convenient is by thermal annealing of silicon rich-oxide (SiO_x, $0 < x < 2$). Its advantage is that it can be produced by completely CMOS compatible methods. Among these methods the LPCVD (Low Pressure Chemical Vapor Deposition) method is known to produce films of very high surface quality, a requirement which is essential for the films employed in the optoelectronics industry. Upon annealing of silicon-rich oxides at high temperatures (800–1100 °C) the excess of silicon groups into nanocrystalline particles (nc-Si). The luminescence of such nanoparticles is strongly dependent on the nanoparticle sizes. Raman spectroscopy can be used to determine the nanoparticle size distribution inside a given sample from the shape and position of both the acoustical[2] and optical phonon peaks.[3–5] In this paper we present a study of nc-Si produced by thermal annealing of the LPCVD produced silicon-rich oxide thin film.

EXPERIMENTAL

The silicon-rich oxide thin films were deposited using the LPCVD method on both silicon and silica substrates. Oxygen and silane diluted in argon (26 % SiH_4, 74 % Ar) were used as reactant gasses. The depositions were made at the temperature of 570 °C and the time of each deposition was 5 hours. The chamber partial pressure and gas flow of silane were kept constant at 22 Pa and 260 cm^3 min^{-1}, respectively. The flow of oxygen was varied to obtain films with different oxygen contents x. The thickness of the SiO_x films determined by m-line measurements is reported in Table 1. The samples were annealed at temperatures of 800, 900, 1000, and 1100 °C for 1 hour in a nitrogen atmosphere to induce the thermal decomposition of SiO_x into nanocrystalline silicon embedded in an amorphous SiO_x matrix. The nitrogen atmosphere was chosen to prevent the further oxidation of our thin films which would take place if the samples were annealed in air. The samples were studied using an Horiba Jobin Yvon T6400 Raman spectrometer. The 514.5 nm line of the argon laser was used for the excitation of the samples.

Table 1. Deposition rate and layer thickness *vs.* O_2 flow

$v(O_2)$ / cm^3 min^{-1}	d / nm	deposition rate / nm min^{-1}
9	378	1.72
13.5	114	1.26
18	127	0.42

[†] Presented at the 34th International Convention on Information and Communication Technology, Electronics and Microelectronics, May 23rd – 27th, 2011, Opatija, Croatia.

* Author to whom correspondence should be addressed. (E-mail: ivanda@irb.hr)

THEORY

To determine the size distribution of nanoparticles in a given matrix from the Raman spectra two different approaches can be used, involving optical and acoustical phonon modes of the nanoparticle, respectively. The phonon confinement model is based on the effect of the change of the shape and position of the optical phonon peak with the decrease of the nano-particle size.[3,4] The spatial confinement of the vibration inside the nanoparticle leads to the breakdown of the momentum conservation rule so that all the phonons down the phonon branch contribute to the Raman spectrum. To model this effect a quantum confinement function which describes the confinement of the optical phonon inside the nanoparticle is used. In this paper we use the following confinement function:[6]

$$W(\vec{r}, D) = \frac{\sin(2\pi r / D)}{2\pi r / D} \quad (1)$$

where D is the diameter of the particle. The contribution of an optical phonon inside the Brillouin zone to the Raman spectrum is given by the Fourier transform of the confinement function. The complete spectrum of the optical phonon is given by the sum of the contributions of all the optical phonons inside the Brillouin zone:

$$I(\omega, D) = \frac{n(\omega) + 1}{\omega} 4\pi \int \frac{\left| \int W(\vec{r}, D) e^{-i\vec{k}\vec{r}} d\vec{r} \right|^2}{[\omega - \omega(k)]^2 + (\Gamma / 2)^2} k^2 dk \quad (2)$$

where the integration is carried out over the entire Brillouin zone, $n(\omega)$ is the Bose-Einstein distribution, Γ is the intrinsic optical phonon peak width (the measured width of the monocrystalline silicon optical phonon peak on our Raman spectrometer is $\Gamma = 3.7$ cm^{-1}) and $\omega(k)$ is the optical phonon dispersion relation (in this paper we used the Brout sum method to average the three optical phonon branches).[7] The convolution of the Raman intensity of a given particle size with the size distribution of particles in the sample gives the final shape of the optical phonon peak. In this paper we used the log-normal distribution to simulate the size distribution of particles in the sample:

$$N(D) = \exp\left[-\frac{(\ln(D / D_0))^2}{2\sigma^2} \right] \quad (3)$$

where D_0 is the mean diameter of the particle and σ is the width of the log-normal distribution.

The low frequency acoustic modes method correlates the position of the low frequency acoustical phonon peaks of the silicon nanoparticle with the mean diameter of the particle. To calculate this correlation the
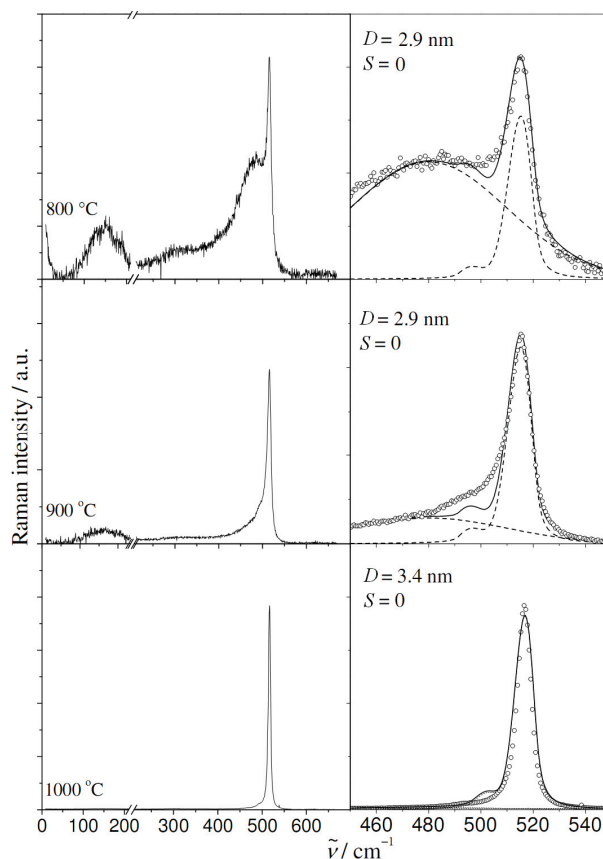

Figure 1. The HV Raman spectra of the annealed sample deposited with the flow of oxygen equal to 9 cm^3 min^{-1}.

nanoparticle is approximated by a homogenous elastic sphere.[8] The normal modes of the sphere naturally group into two distinct groups: the torsional and the spheroidal modes. The spheroidal and torsional modes are classified according to the symmetry group of the sphere by labels (l, m) as for the spherical harmonics Y_{lm}, only the $l = 0$ and $l = 2$ modes being Raman active.[9] The $l = 0$ mode is purely symmetrical and is present only in the HH (incident light horizontally polarized, scattered light horizontally polarized) spectrum, while the $l = 2$ mode is present in both the HV (incident light horizontally polarized, scattered light vertically polarized) and HH spectra, although in the HH spectrum the dominant mode is usually the $l = 0$ mode. The position of the $l = 0$ peak is inversely proportional to the mean diameter of the nanoparticle and for a free particle is given by:

$$\nu D_0 = S \frac{v_l}{c} \quad (4)$$

where ν is the acoustical mode wavenumber, D_0 is the diameter of the particle, S is a constant of the order of unity which depends only on the Poisson's ratio of the nanoparticle and the mode labels (l, m), v_l is the longitudinal velocity of sound in the particle and c is the speed
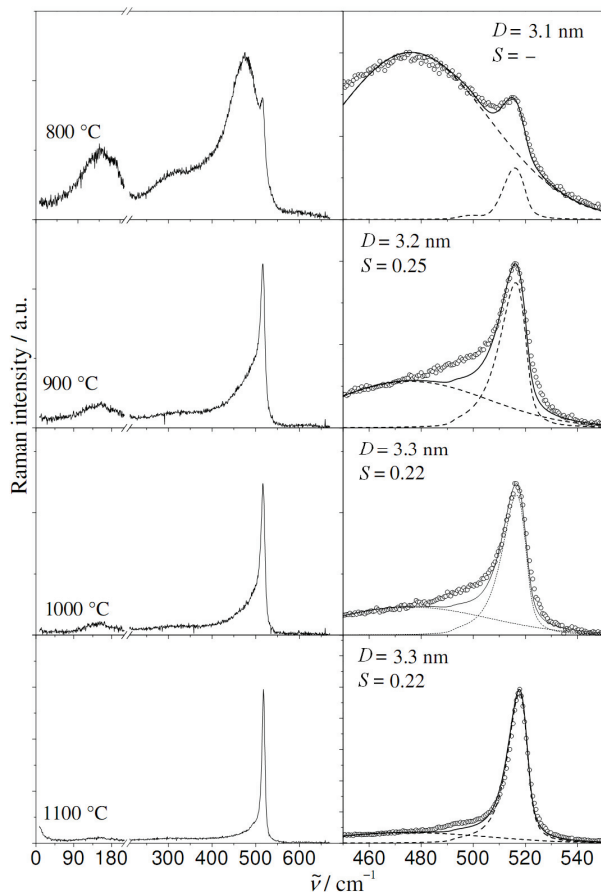
Figure 2. The HV Raman spectra of the annealed sample deposited with the flow of oxygen equal to 13.5 cm^3 min^{-1}.

Figure 3. The HV Raman spectra of the annealed sample deposited with the flow of oxygen equal to 18 cm^3 min^{-1}.

of light. Since silicon is highly anisotropic and the above-mentioned model is valid only for isotropic materials, averaged values of the longitudinal and transversal sound velocities in silicon were taken to calculate the coefficient S. Values of $v_l = 8790$ m s^{-1} and $v_t = 5410$ m s^{-1} which give a Poisson's ratio of 0.195 were used. The calculated value of S for the $l = 0$ mode of silicon is $S = 0.78$.

RESULTS

The HV Raman spectra of the samples deposited with the flows of oxygen equal to 9, 13.5 and 18 cm^3 min^{-1} are reported in Figures 1, 2, and 3, respectively. The left part of the all three figures shows the complete Raman spectrum from 0 to 700 cm^{-1} where the region from 0 to 210 cm^{-1} is the spectrum of the sample deposited on the silicon, and the region from 210 to 700 cm^{-1} on the silica substrate. This was done to avoid the contribution of the Raman spectrum of the substrate to the Raman spectrum of the film, since the samples are very thin. The crystalline silicon which was used for the substrate has a strong peak at 520 cm^{-1} corresponding to the optical phonon peak, while in the region between 0–210
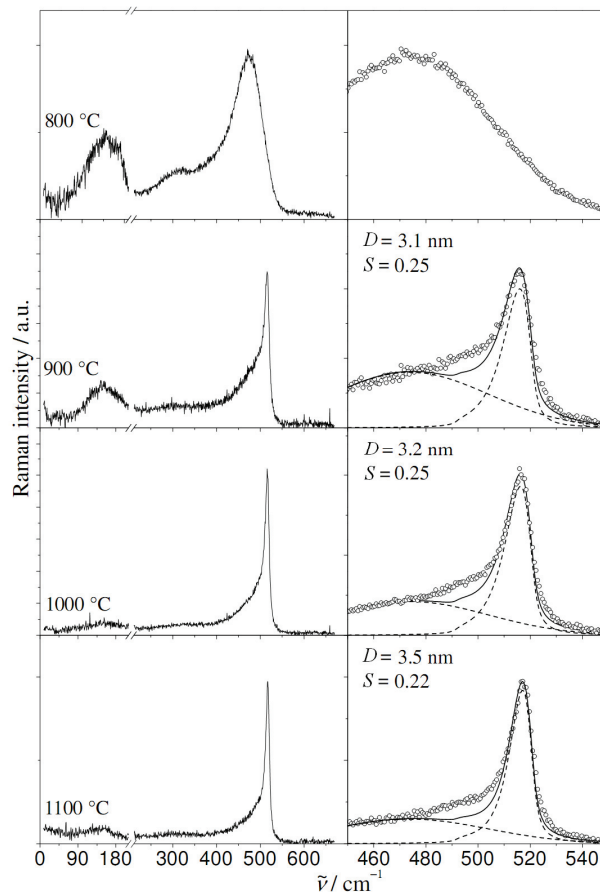
cm^{-1} is without any features. Pure silica on the other hand in the HV spectrum has a strong peak in the region around 50 cm^{-1}, while it is without any features in the area from 210–700 cm^{-1}. By combining the two spectra as shown in Figures 1–3 we can reproduce the pure spectra of SiO$_x$ thin films. The right part of the Figures 1–3 is the enlarged area of the silicon optical phonon peak from 450 to 550 cm^{-1}. The circles represent the experimental spectra. The dashed lines are the optical phonon mode peak profile, calculated from the phonon confinement model (2) and the broad band of the amorphous SiO$_x$ matrix. The full line is the sum of the two dashed lines. For all samples two distinctive features can be seen in the enlarged region of the Raman spectra between 450 and 550 cm^{-1} which is presented in the right part of Figures 1–3: the broad band of the amorphous SiO$_x$ matrix (a-SiO$_x$) centered between 470–480 cm^{-1}, and the nano-crystalline silicon (nc-Si) peak between 510–520 cm^{-1}. Higher the annealing temperature, higher the intensity of the nc-Si peak in respect to the intensity of the a-SiO$_x$ band. Also the position of the nc-Si peak shifts slightly towards higher wavenumbers. For the samples annealed at 800 °C the silicon crystalline peak is clearly visible for the sample with $v($O$_2) = 9$ cm^3

Table 2. The fitting parameters for the samples deposited under different flows of oxygen $v(O_2)$ and annealed at different temperatures T: the mean particle diameter D_0, the width of the lognormal distribution σ, the ratio of the intensities of the a-SiO$_x$ and the nc-Si peaks and the position of the a-SiO$_x$ band. The width of the a-SiO$_x$ band was found to be 30 cm^{-1} for all the samples

$v(O_2)$ / cm^3 min^{-1}	T / C	D_0 / nm	σ	I(a-SiO$_x$) / I(nc-Si)	v(a-SiO$_x$) / cm^{-1}
	800	2.9	< 0.1	0.72	
9	900	2.9	< 0.1	0.13	480
	1000	3.4	< 0.1	0.03	
	800	3.1	–	3.2	
13.5	900	3.2	0.25	0.32	476
	1000	3.3	0.22	0.2	
	1100	3.8	0.2	0.07	
	800	–	–	–	
18	900	3.1	0.25	0.4	474
	1000	3.2	0.25	0.23	
	1100	3.5	0.22	0.16	

min^{-1}, barely visible for the sample with $v(O_2) = 13.5$ cm^3 min^{-1} and completely overshadowed by the much more broad a-SiO$_x$ band for the sample with $v(O_2) = 18$ cm^3 min^{-1}. This is because the higher the silicon concentration, the higher will be the concentration of silicon nanoparticles, and therefore the intensity of the crystalline silicon peak will also be higher. The experimental spectra were fitted using the phonon confinement model. For the broad a-SiO$_x$ band a Gaussian function was used to represent it. The Gaussian functions representing the a-SiO$_x$ band were determined from the spectra of the samples annealed at 800 °C (where the a-SiO$_x$ band is the most intense) and the same function was used to fit all the samples of the same series. The nc-Si peak was fitted using the phonon confinement model (2) where the mean particle diameter D_0 and the width of the lognormal distribution σ were used as fitting parameters. The results of the fit are summarized in Table 2.

The increase of the nano-particle mean diameter with the increase of the annealing temperature is evident for all three series of samples. For the sample with $v(O_2) = 9$ cm^3 min^{-1} the width of the lognormal distribution is very small which implies a homogenous distribution of particle sizes in the sample, while for samples deposited with higher flows of oxygen into the reactor the width of the lognormal distribution is between 0.2–0.25. For the sample with $v(O_2) = 9$ cm^3 min^{-1} and $T = 800$ °C the nc-Si peak has a very low intensity so it was impossible to determine the σ. For all samples a clear disagreement between the experimental spectra and the theoretical fit is evident in the area between 490–510 cm^{-1} which was also previously observed when the experimental spectra of nc-Si in an SiO$_x$ matrix were fitted using the phonon confinement model.[3,4]

The disagreement was explained either by the effect of stress on the nc-Si particle[10] or by the existence of two different size distributions of particles in the samples.[11] A possible explanation of the disagreement is that it is caused by the limitations of the phonon confinement model itself. The phonon confinement model supposes that the optical phonon wavevector is completely radial to the surface of the sample (in Equation (1) the phonon confinent function is purely radial). This approximation is not valid for small nanoparticles since with the decrease of the nanoparticle size, the part of the wavevector tangential to the surface of the sample will tend to be quantisied. Because of the spherical symmetry of the nanoparticle such modes can be generally described by the spherical harmonics and quantisied by the quantum numbers l and m. The optical mode described by the phonon confinement model is only the purely radial $l = 0$ mode. The $l = 1, 2, 3...$ modes will have a zone-center wave-vector value larger than zero since in addition to the radial component (equal to zero at zone-centre) they will have also an angular component. Since the optical phonon dispersion of silicon generally slopes toward lower phonon energies when the wavevector increases (when moving from the centre

Table 3. The position of the low frequency acoustical mode peak and the diameter of the nanoparticle calculated from the position of the peak for samples whose production parameters are given in the table

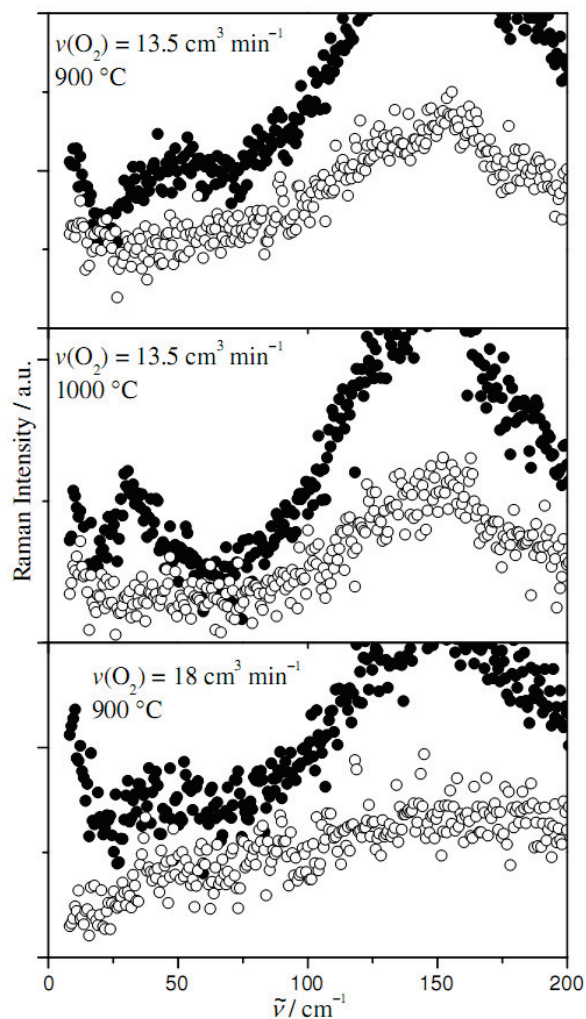| $v(O_2)$ / cm^3 min^{-1}	T / °C	v / cm^{-1}	D_0 / nm
13.5	900	46	5
13.5	1000	32	7.1
18	900	40	5.7

Figure 4. The HH (full circles) and HV (open circles) Raman spectra of the samples whose parameters of deposition are given in the inset.

of the Brilloiuon zone towards its edge) the $l = 1, 2, 3...$ modes will be found at lower energy values than the $l = 0$ mode. Each of this modes will generally also be shifted and broadened by the radial confinement as described by the phonon confinement model for the $l = 0$ mode. Therefore the structure around 490–500 cm^{-1} can be explained by the presence of the $l = 1$ or possibly the $l = 2$ mode. A detail study of such phenomena will be reported elsewhere.[12] As for the position od the a-SiO$_x$ band a small shift from 480 to 474 cm^{-1} was found when increasing the oxygen content in the samples, probably caused by the increase of the internal strain inside the matrix due to the increase of the oxygen content.

The low frequency part of the Raman spectra of the sample deposited with $v(O_2) = 13.5$ cm^3 min^{-1} annealed at 900 °C and at 1000 °C and of the sample deposited with $v(O_2) = 18$ cm^3 min^{-1} annealed at 900 °C deposited on silicon substrates are shown in Figure 4. A clear difference between the HH and HV spectra in the

region between 0 and 100 cm^{-1} is observed. In the HH spectra of all three samples there is a peak clearly visible between 30 and 50 cm^{-1} which we attribute to the $l = 0$ acoustical mode. The positions of these peaks and from them calculated values of the particle diameters are shown in Table 3. The low frequency acoustical modes method seems to give systematically higher values of nanoparticle mean sizes than the phonon confinement model. A possible explanation is that the silicon nanoparticles inside an SiO$_x$ matrix are not completely crystalline but have a crystalline core and an amorphous silicon shell.[13] The amorphous shell would have a greater effect on the optical than on the acoustical mode, since the high wavevector (small wavelength) optical mode would be much more quickly damped in the amorphous shell than the low wavevector (high wavelength) acoustic mode. Therefore the effective size of the particle determined from the optical modes is expected to be lower than the size determined from the acoustical modes.

CONCLUSION

Thin silicon rich oxide films were deposited using the LPCVD method, and were later annealed at temperatures of 800, 900, 1000, and 1100 °C in order to induce the thermal decomposition of the silicon rich oxides into nanocrystalline silicon inside an amorphous matrix. Raman spectroscopy has found that the crystallization of silicon into nanoparticles takes place, and that the size of the particles increases with the increase of temperature. The size of the particles was found to be around 3 nm by the phonon confine-ment model (possibly the crystalline core of the particles) and from 5–7 nm by the low frequency acoustical modes model (possibly the whole, not necessarily crystalline, silicon conglomeration inside the silicon rich oxide matrix).

REFERENCES

1. L. Pavesi, L. Dal Negro, C. Mazzoleni, G. Franzò, and F. Priolo, *Nature* **408** (2000) 4410.
2. M. Fujii , T. Nagareda, S. Hayashi, and K. Yamamoto, *Phys. Rev. B* **54** (1969) R8373.
3. H. Richter, Z. P. Wang, and L. Ley, *Solid State Commun.* **36** (1981) 625.
4. P. H. Fauchet and I. H. Campbell, *Crit. Rev. Solid State Mater. Sci.* **14** (1988) S79.
5. I. H. Campbell and P. M. Fauchet, *Solid State Commun.* **39** (1981) 625.

6. V. Paillard, P. Puech, M. A. Laguna, and R. Carles, *J. Appl. Phys.* **86** (1999) 1921.
7. R. Brout, *Phys. Rev.* **113** (1959) 43.
8. H. Lamb, *Proc. London Math. Soc.* **S1-13** (1881) 189.
9. E. Duval, *Phys. Rev. B* **46** (1992) 5795.
10. D. Ristić, M. Ivanda, and K. Furić, *J. Mol. Struct.* **924** (2009) 291.
11. A. Gajović, D. Gracin, K. Juraić, J. Sancho-Parramon, and M. Čeh, *Thin Solid Films* **517** (2009) 5453.
12. M. Mattarelli, M. Montagna, D. Ristić, and M. Ivanda, unpublished.
13. M. Ivanda, A. Hohl, M. Montagna, G. Mariotto, M. Ferrari, Z. Crnjak Orel, A. Turković, and K. Furić, *J. Raman Spectrosc.* **37** (2006) 161–165.